Inorganic Chemistry

ARTICLE

pubs.acs.org/IC

Zinc Paddlewheel Dimers Containing a Strong $\pi\cdots\pi$ Stacking Supramolecular Synthon: Designed Single-Crystal to Single-Crystal Phase Changes and Gas/Solid Guest Exchange

Daniel L. Reger,* Agota Debreczeni, and Mark D. Smith

Department of Chemistry and Biochemistry, University of South Carolina, Columbia, South Carolina 29208, United States

Supporting Information

ABSTRACT: The ligand 4-(1,8-naphthalimido)benzoate, $\mathbf{L_{C4}}^-$, containing a linear link between the strong $\pi\cdots\pi$ stacking 1,8-naphthalimide supramolecular synthon and the carboxylate donor group, reacts with $Zn(O_2CCH_3)_2(H_2O)_2$ in the presence of dimethylsulfoxide (DMSO) to yield $[Zn_2(\mathbf{L_{C4}})_4(DMSO)_2]\cdot 2(CH_2Cl_2)$. This compound contains the "paddlewheel" $Zn_2(O_2CR)_4$ secondary building unit (SBU) that organizes the rigid phenylene and naphthalimide rings of the carboxylate ligands in a square arrangement. The supramolecular architecture is dominated by $\pi\cdots\pi$ stacking interactions between naphthalimide rings of one dimer with four adjacent dimers, essentially at right angles, forming an open three-dimensional network structure. Two symmetry equivalent networks of this type interpenetrate generating overall a densely packed three-dimensional, 2-fold interpenetrated architecture in which the CH_2Cl_2 solvate molecules are trapped in isolated pockets. Upon cooling, single crystals of $[Zn_2(\mathbf{L_{C4}})_4(DMSO)_2]\cdot 2(CH_2Cl_2)$ undergo two distinct crystallographic phase transitions, as characterized by X-ray diffraction at different temperatures, without loss of crystallinity. These two new phases have supramolecular structures very similar to the room temperature structure, but changes in the ordering of the CH_2Cl_2 solvate cause shifting of the naphthalimide rings and a lowering of the symmetry. Crystals of $[Zn_2(\mathbf{L_{C4}})_4(DMSO)_2]\cdot 2(CH_2Cl_2)$ undergo a single-crystal to single-crystal gas/solid guest exchange upon exposure to atmospheric moisture, or faster if placed under vacuum or heated under dry gas to 100 °C, followed by atmospheric moisture, to yield $[Zn_2(\mathbf{L_{C4}})_4(DMSO)_2]\cdot 3.9(H_2O)$. The molecular and supramolecular structures of this new compound are very similar to the dichloromethane adduct, with now the water molecules encapsulated into the framework. The remarkable feature of both the phase changes and exchange of solvates is that this robust network is not porous; local distortions (ring slippage and tilting changes) of the $\pi\cdots\pi$ stacking interactions of the naphthalimide rings that organize these structures allow these changes to take place without the loss of crystallinity. The complexes $[Zn_2(\mathbf{L_{C4}})_4(DMSO)_2]\cdot 2(CH_2Cl_2)$ and $[Zn_2(\mathbf{L_{C4}})_4(DMSO)_2]\cdot 3.9(H_2O)$ show green emission in the solid state.

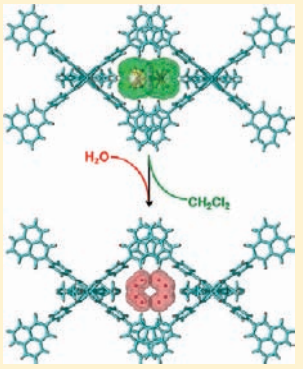

INTRODUCTION

Crystal engineering of framework materials built from metal centers linked by organic spacers has become of great interest in the field of chemistry and materials science. Such interest in these materials can be attributed to the possibility of designing various properties and functions into these solids for promising applications in catalysis,[1] energy storage,[2] sensing,[3] and separation.[4]

Extensive research has been dedicated to the construction of porous crystalline architectures connecting rigid metallic building blocks, referred as secondary building units (SBUs), with robust organic linkers via strong covalent bonds, compounds generally referred as metal−organic frameworks (MOFs).[5] The use of multidentate carboxylate ligands as the organic linkers to join the metallic SBU cores allows the formation of rigid frameworks, with a particular advantage in many cases that neutral open networks can be produced in which no counterions are needed to achieve electroneutrality.[5]

Metal complexes of linked monodentate ligands (using mostly rigid pyridine-based compounds) have been used to prepare hybrid organic−inorganic materials containing large voids, usually filled with solvent molecules.[6] These species can be viewed as different from MOFs in the sense that in some cases the stability of the framework is reduced, and the network collapses upon the removal of solvent molecules.[6d,e]

Less rigid, but still highly organized structures can be assembled by noncovalent forces, with hydrogen bonding being the predominant organizational synthon due to its reproducible and directionality properties.[7] Recently, increased attention has been dedicated to employ hydrogen bonding in the assembly of flexible hybrid frameworks containing dynamic pores, which can possess more "elastic" properties than rigid three-dimensional networks, opening the field for the design of a new class of practical materials.[8] Other noncovalent interactions, predominantly $\pi\cdots\pi$ stacking between aromatic rings, have also been used in the assembly of "soft" crystalline solids.[9] Although, this interaction is not as directional as hydrogen bonding, an order of stability in the interaction of two π systems has been well

Received: August 22, 2011
Published: October 27, 2011

Scheme 1. Bifunctional Carboxylate Ligands

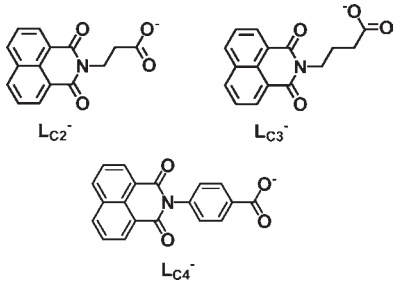

established: π-deficient − π-deficient > π-deficient − π-rich > π-rich − π-rich, where the stronger interactions can be a force of similar robustness to hydrogen bonding in a properly chosen aromatic system.[10]

In the past few years, our group has exploited the unusually strong $\pi\cdots\pi$ stacking interactions of the π-deficient 1,8-naphthalimide group (see Scheme 1) within different metal complexes. In our initial studies, it was shown that this naphthalimide moiety incorporated into bis(pyrazolyl)methane[11a] and 2,2′-bipyridine[11c] ligand systems leads to association into dimers of metal complexes of the ligands. Importantly, we were able to demonstrate that the strong π-association of the naphthalimide rings not only is observed in the solid state but also persist in solution.[11] In addition, we have shown that $\pi\cdots\pi$ stacking of this functional group leads to the formation of silver(I) coordination polymers with interesting structures.[11b]

Recently, we have prepared bifunctional carboxylate ligands that contain both the carboxylate donor group and the 1,8-naphthalimide π-stacking synthon (Scheme 1), in order to assemble three-dimensional, MOF like architectures that combine the robustness of transition metal-carboxylate SBU cores with the supramolecular organization given by the 1,8-naphthalimide rings. We have termed these solids supramolecular metal−organic frameworks (SMOFs), framework solids with a three-dimensional structure in which the building blocks are organized partially or completely by robust supramolecular interactions. In our initial work, the two carboxylate ligands $\mathbf{L_{C2}}^-$ and $\mathbf{L_{C3}}^-$, pictured in Scheme 1, were prepared and incorporated into the paddlewheel $Cu_2(O_2CR)_4$ type SBU core.[11d] Structural investigations of these complexes demonstrated the formation of high dimensionality materials, organized partially or completely by the strong π-association of the 1,8-naphthalimide rings. Although highly organized, the supramolecular structures of complexes of these two ligands were not dominated by the "square" arrangement of the paddlewheel SBU because the two or three sp^3 hybridized carbon centers that link the carboxylate donor and the naphthalimide groups do not necessarily enforce this geometry.

Reported here are the synthesis and properties of new tetracarboxylato dizinc complexes that combine the $\mathbf{L_{C4}}^-$ bifunctional ligand (Scheme 1) with the robust $Zn_2(O_2CR)_4$ paddlewheel unit. We are particularly interested in the chemistry of $\mathbf{L_{C4}}^-$ because the rigid, linear arrangement of the linking phenylene group enforces the "square" architecture of the paddlewheel SBU on the positions of the naphthalimide supramolecular synthons and, in addition, should promote the formation of more "open" structures. Using noncovalent interactions to organize the square metallic SBU cores, a unique three-dimensional robust framework is obtained that has "local flexibility" due to the $\pi\cdots\pi$ stacking interactions. Particularly interesting features of these solids are the single-crystal to single-crystal exchange of small guest molecules in a gas/solid-mediated transformation as well as temperature induced phase changes. The new solids also show luminescent behavior.

EXPERIMENTAL SECTION

General Considerations. All reactants were used as purchased from Aldrich. The IR measurements were carried out on ground crystals using a Perkin-Elmer FTIR 100 spectrometer with the attenuated total reflectance (ATR) accessory. The reflectance measurements were done on a Perkin-Elmer Lambda 35 UV−vis spectrometer using the Labsphere RSA-PE-20 reflectance spectroscopy accessory. The fluorescence spectra were recorded on a Perkin-Elmer LS 55 fluorescence spectrometer. Ground solid samples were used in a 6 nm cell. Thermogravimetric analysis (TGA) was performed using a Thermal Analysis (TA) SDT-Q600 simultaneous differential thermal analysis (DTA)/TGA system. The sample was heated in air to 800 °C with a heating rate of 10 °C/min. In the single-crystal to single-crystal transformation experiments, in each cycle, the sample was heated at the rate of 0.5 °C/min until 100 °C and was held isothermal at that temperature for 15 min; after this period, the sample was cooled to 25 °C and held isothermal at that temperature for 48 h. The in situ X-ray diffraction study was performed using a hot-stage-equipped Rigaku D/Max 2100 powder diffractometer using Cu Kα radiation. Data were collected at a 0.02° step for 4.8 s/step over the 2θ range 5−30°. The protonated form of the ligand, 4-(1,8-naphthalimido)benzoic acid ($H\mathbf{L_{C4}}$), was synthesized as previously reported.[11i] Elemental analyses were performed by Robertson Microlit Laboratories (Ledgewood, NJ).

Synthesis of $[Zn_2(L_{C4})_4(DMSO)_2]\cdot 2(CH_2Cl_2)$. $H\mathbf{L_{C4}}$ (0.064 g, 0.20 mmol) was dissolved in 2 mL of dimethylsulfoxide, and then, 20 mL of dichloromethane was added. $Zn_2(O_2CCH_3)_2(H_2O)_2$ (0.022 g, 0.10 mmol) was dissolved in methanol (20 mL). Equal aliquots of each solution were divided into three test tubes (dichloromethane solution added first) with a buffer layer of pure methanol (6 mL) placed between the two solutions. The test tubes were stored undisturbed at room temperature, yielding, after a few days, X-ray quality crystals. Yield: 0.057 g (0.033 mmol, 66%). The analytical sample was dried to constant weight, Anal. Calcd. (Found) for $C_{80}H_{52}Zn_2N_4O_{18}S_2$ (without solvent of crystallization): C 61.90 (61.65); H 3.38 (3.43); N 3.61 (3.51). IR (cm^{-1}): ν_{CO} = 1705 (m), 1643 (s), 1584 (m), 1402 (s), 1373 (m), 1353 (s); ν_{SO} = 962 (m).

Synthesis of $[Zn_2(L_{C4})_4(DMSO)_2]\cdot 3.9(H_2O)$. Crystals of $[Zn_2(\mathbf{L_{C4}})_4(DMSO)_2]\cdot 2(CH_2Cl_2)$ were placed under high vacuum for 5 days and then were exposed to atmospheric moisture for 5 days. X-ray diffraction showed that these crystals were now $[Zn_2(\mathbf{L_{C4}})_4(DMSO)_2]\cdot 3.9(H_2O)$. Anal. Calcd. (Found) for $[Zn_2(\mathbf{L_{C4}})_4(DMSO)_2]\cdot 3.9(H_2O)$ ($C_{80}H_{59.8}Zn_2N_4O_{21.9}S_2$): C 59.22 (59.41), H 3.72 (3.58), N 3.45 (3.34). IR (cm^{-1}): ν_{OH} = 3474 (b), ν_{CO} = 1704 (m), 1643 (s), 1583 (m), 1401 (s), 1373 (m), 1352 (s); ν_{SO} = 961 (m).

Crystallographic Studies. Crystals form as well-faceted yellow prisms up to ca. 1 mm in size. The crystals variously grow with a block, plate, or rod habit. In air, fine cracks appear in the crystals on a time scale of tens of minutes, presumably as a result of the guest−molecule exchange process taking place (see below). Crystallinity is not adversely affected by this process. Temperature-dependent phase transition behavior was identified after room-temperature data and 150 K data sets gave different unit cells. Subsequently, multiple data sets consisting of three 25-frame scans at orthogonal crystal orientations were collected to determine transition temperatures. This procedure was performed by initially cooling from 295 to 110 K in increments of ca. 25°, followed by warming to room temperature, and then cooling in smaller increments (3°) in the area of the transition points bracketed by the first cooling run.

dx.doi.org/10.1021/ic201830h |Inorg. Chem. 2011, 50, 11754–11764

Table 1. Selected Crystallographic Data for $[Zn_2(L_{C4})_4(DMSO)_2]\cdot 2(CH_2Cl_2)$ at Three Different Temperatures

	295 K	250 K	110 K
formula	$C_{82}H_{56}Cl_4N_4O_{18}S_2Zn_2$	$C_{82}H_{56}Cl_4N_4O_{18}S_2Zn_2$	$C_{82}H_{56}Cl_4N_4O_{18}S_2Zn_2$
fw, g mol^{-1}	1721.97	1721.97	1721.97
cryst. syst.	orthorhombic	monoclinic	monoclinic
space group	*Cmca*	*C*2/*c*	$P2_1/n$
T (K)	295	250	110
a, Å	28.488(2)	28.332(3)	16.8397(16)
b, Å	18.4743(13)	18.5103(17)	13.9012(14)
c, Å	14.0764(10)	14.0046(12)	16.8551(16)
α, deg	90	90	90
β, deg	90	92.769(2)	113.631(2)
γ, deg	90	90	90
V, Å^3	7408.5(9)	7335.8(11)	3614.8(6)
Z	4	4	2
R_1 $I > 2\sigma(I)$	0.0529	0.0576	0.0326
wR_2 $I > 2\sigma(I)$	0.1468	0.1394	0.0851
R (int)	0.0478	0.0810	0.0355

The phase transitions are reversible; the diffraction pattern behavior is identical upon warming or cooling.

All X-ray intensity data were measured using a Bruker SMART APEX diffractometer (Mo Kα radiation, λ = 0.71073 Å).[12] The raw area detector data frames were reduced and corrected for absorption effects with the SAINT+, SADABS, and TWINABS programs.[12] Unit cell parameters were determined by least-squares refinement of large sets of strong reflections from the data sets. Direct methods structure solution, difference Fourier calculations, and full-matrix least-squares refinement against F^2 were performed with SHELXTL.[13] In general, all nonhydrogen atoms were refined with anisotropic displacement parameters except where noted. Hydrogen atoms were placed in geometrically idealized positions and refined as riding atoms. X-ray crystallographic data are given in Table 1.

295 K. The data crystal was encased in epoxy glue to protect against guest molecule exchange. At 295 K, the reduced unit cell parameters are *a* = 14.076 Å, *b* = 16.977 Å, *c* = 16.977 Å, α = 65.93°, β = 90°, and γ = 90°, which transform into an orthorhombic *C*-centered Bravais lattice with cell constants *a* = 28.488(2) Å, *b* = 18.4743(13) Å, *c* = 14.0764(10) Å, *V* = 7408.5(9) Å^3. The space group *Cmca* (No. 64) was determined by the pattern of systematic absences in the intensity data and by the successful refinement model. The asymmetric unit consists of 1/4 of one dizinc complex and half of one dichloromethane molecule. The dizinc complex is situated about a site with 2/m (C_{2h}) point symmetry. The zinc atom resides on a mirror plane. There is one independent $\mathbf{L_{C4}}^-$ ligand. The coordinated dimethylsulfoxide (DMSO) molecule is disordered across the mirror plane and was refined with half occupancy. The two independent sulfur−carbon distances were restrained to be similar (SHELX SADI instruction). The dichloromethane molecule is also disordered across the mirror plane, with the carbon atom in the plane. The chlorine atoms are further disordered over three independent positions *A*/*B*/*C* in the asymmetric unit and were refined with fixed occupancies *A*/*B*/*C* = 0.5/0.25/0.25. The occupancies were initially refined to values close to those reported and were subsequently fixed for refinement stability. Carbon−chlorine distances were restrained to 1.75(2) Å. The carbon atoms of the disordered DMSO and dichloromethane molecules were refined isotropically.

250 K. Upon cooling of the crystal, splitting of the diffraction peaks is observed starting at ca. 265 K. The splitting becomes further resolved in the range 260−240 K and then is observed to coalesce again upon further cooling. The evolution of a diffraction peak profile is shown in Figure S1 (Supporting Information) to illustrate the change. Data for this phase were collected at 250 K. Analysis of the 250 K data set shows the crystal is now twinned by nonmerohedry with two domains. The diffraction pattern can be completely indexed using two *C*-centered monoclinic cells with lattice parameters *a* = 28.332(3) Å, *b* = 18.5103(17) Å, *c* = 14.0046(12) Å, β = 92.769(2)°, and *V* = 7335.8(11) Å^3. This unit cell corresponds to reduced cell parameters of *a* = 14.005 Å, *b* = 16.921 Å, *c* = 16.921 Å, α = 66.32°, β = 87.68°, and γ = 87.68°. The two twin domains are related to one another by a 180° rotation about the reciprocal [100] axis, corresponding in real space to the [1 0 −0.04] axis. The twin law derived by the program CELL_NOW is, by rows, (1 0 0.08/0 −1 0/−0.03 0 −1), which was also used for generation of orientation matrices for both domains.[14] The small nonzero twin matrix elements reflect the small peak splitting observed in the diffraction pattern, i.e., the two domains are nearly in registry. The space group was eventually determined to be *C*2/*c* (No. 15), which is a maximal nonisomorphic subgroup (Type I, index 2) of the room-temperature space group *Cmca*. Data were refined in SHELX using an HKFL5 format reflection file, which was created using the TWINABS program.[12] The major twin fraction refined to 0.671(2). The asymmetric unit in *C*2/*c* consists of half of one dizinc complex and one dichloro methane molecule. The dizinc complex is situated on an inversion center. There are two independent $\mathbf{L_{C4}}^-$ ligands. The DMSO molecule is disordered over two general positions in the ratio S1A/S1B = 0.643(3)/0.357(3), with the total population constrained to sum to unity. The dichloromethane molecule is disordered over three general positions with refined occupancies *A*/*B*/*C* = 0.647(3)/0.128(4)/0.225(4), also constrained to sum to unity. Disordered carbon atoms and the minor chlorine atoms (component B) were refined isotropically. A total of 22 distance restraints were used to maintain chemically reasonable geometries for the disordered species.

110 K. On cooling from 250 K, the split diffraction peaks coalesce and become single maxima again near 195 K. This unusual observation implies that the two twin domains related by nonmerohedry have reoriented and are now in registry (their diffraction patterns overlay). The diffraction pattern can be fully indexed to give a reduced unit cell with parameters *a* = 13.86 Å, *b* = 13.86 Å, *c* = 16.80 Å, α = 66.27°, β = 90°, and γ = 90°. This unit cell closely corresponds to the reduced unit cell of the room temperature orthorhombic form (see Figure S1, Supporting Information). For comparison, the *C*-centered orthorhombic cell corresponding to these reduced parameters is *a* = 18.40 Å, *b* =

dx.doi.org/10.1021/ic201830h |*Inorg. Chem.* 2011, 50, 11754–11764

Table 2. Selected Crystallographic Data for $[Zn_2(L_{C4})_4(DMSO)_2]\cdot n(H_2O)$

	$[Zn_2(L_{C4})_4(DMSO)_2]\cdot 2.34(H_2O)$	$[Zn_2(L_{C4})_4(DMSO)_2]\cdot 3.92(H_2O)$
formula	$C_{80}H_{56.67}N_4O_{20.34}S_2Zn_2$	$C_{80}H_{59.84}N_4O_{21.92}S_2Zn_2$
fw, g mol^{-1}	1594.23	1622.74
cryst. syst.	orthorhombic	orthorhombic
space group	*Cmca*	*Cmca*
T (K)	294	294
a, Å	28.538(3)	28.6556(14)
b, Å	18.3527(17)	18.2788(9)
c, Å	13.7243(13)	13.6636(7)
α, deg	90	90
β, deg	90	90
γ, deg	90	90
V, Å^3	7188.2(12)	7156.9(6)
Z	4	4
R_1 $I > 2\sigma(I)$	0.0472	0.0468
wR_2 $I > 2\sigma(I)$	0.1378	0.1393
R (int)	0.0733	0.0585

28.19 Å, c = 13.86 Å, $\alpha = 90°$, $\beta = 90°$, and $\gamma = 89.80°$. This cell is actually given as an option by the SMART indexing software but is rejected because of the gamma angle and more definitively after structure solution. More importantly, trial refinements of the 110 K data in *Cmca* led to disorder of the methylene chloride and DMSO molecules, which is resolved in $P2_1/n$, unreasonable displacement ellipsoids for phenyl ring and solvent atoms, and R-values >15%. The ordering of the CH_2Cl_2 and DMSO molecules makes the structure incompatible with the three mutually perpendicular 2-fold axes that define the orthorhombic system. After transformation to the standard b-unique monoclinic setting, the 110 K form has a primitive monoclinic lattice with a = 16.8397(16) Å, b = 13.9012(14) Å, c = 16.8551(16) Å, β = 113.631(2)°, and V = 3614.8(6) Å^3. In the 110 K phase, the centered Bravais lattice symmetry present above 265 K is broken. Systematic absences in the 110 K data set uniquely determined the space group $P2_1/n$, which is in turn a maximal nonisomorphic subgroup (Type IIa, index 2) of the 250 K space group, $C2/c$. The crystal is now twinned with exchange of the similar a and c axes, with the two domains related by the twin matrix (0 0 −1/0 −1 0/−1 0 0). The diffraction patterns originating from the two domains are superimposed in this form of twinning, and the structure was refined normally in SHELX using the TWIN instruction and the matrix given above. The major twin fraction was refined to 0.578(1). The asymmetric unit in $P2_1/n$ is similar to that in $C2/c$, consisting of half of one centrosymmetric dizinc complex and one dichloromethane molecule, with all species now ordered. The dizinc complex is situated on an inversion center, with one zinc atom, two independent L_{C4}^- ligands, and one DMSO molecule. Examination of the final residual electron density map shows the largest peak of 0.88 e/Å^3 is near the DMSO sulfur atom, indicating some small DMSO disorder fraction still persists. Trial DMSO disorder models indicate the minor disordered fraction is ca. 5%, and it was not modeled.

Hydrated (Solvent Exchanged) Forms. No phase transition behavior was observed in the temperature range 296−110 K. The hydrated form is orthorhombic, with the space group *Cmca* and lattice parameters of $a \sim 28.5$ Å, $b \sim 18.3$, and $c \sim 13.7$, at all accessible temperatures. Each hydrated data set was collected at 294 K. X-ray crystallographic data for hydrated forms are given in Table 2.

The asymmetric unit in *Cmca* is similar to the dichloromethane solvates, consisting of 1/4 of a C_{2h}-symmetric dizinc complex with the zinc atom on a mirror plane and the DMSO disordered across the mirror plane. In the interstitial region, two significant electron density peaks were observed and were modeled as variably occupied oxygen atoms of water molecules. These atoms were assigned a fixed isotropic displacement parameter of U_{iso} = 0.15 Å^2, and their occupancies were freely refined. Free refinement of both the U_{iso} and occupancy values did not result in stable or sensible values. It should be noted that, since atomic site occupancies are strongly correlated with displacement parameters, the uncertainty in the water content derived from the X-ray refinements is likely underestimated. The pattern of interstitial occupancy has a general V-shape, resembling a dichloromethane molecule. Several refinement models using CH_2Cl_2 as the guest were attempted but ultimately rejected because of (1) poor dichloromethane geometry, even if restrained, (2) unacceptably high displacement parameters for the carbon and chlorine atoms, and (3) unreasonably short distances (ca. 2.6 Å) to the closest naphthalimide ring hydrogen (H12). In comparison, the Cl···H nonbonded distance in the 295 K *Cmca* dichloromethane solvate structure (see above) is 2.96 Å, which is greater than the sum of the van der Waals radii for chlorine and hydrogen.[15] The distances observed in the hydrated structures are sensible for a water molecule hydrogen-bonded to a carbonyl oxygen (O1S···O2 = 3.15 Å) and a CH···O interaction with the naphthalimide ring.

RESULTS

The $[Zn_2(L_{C4})_4(DMSO)_2]\cdot 2(CH_2Cl_2)$ complex was prepared by layering a CH_2Cl_2 solution of HL_{C4} containing a small amount of dimethylsulfoxide with a methanol solution of $Zn(O_2CCH_3)_2(H_2O)_2$. The slow diffusion of the layers led to the formation of $[Zn_2(L_{C4})_4(DMSO)_2]\cdot 2(CH_2Cl_2)$ crystals suitable for X-ray diffraction.

Solid State Structure Analysis. Single crystals of $[Zn_2(L_{C4})_4(DMSO)_2]\cdot 2(CH_2Cl_2)$ were characterized by X-ray diffraction at different temperatures because of phase changes, vide infra. A drawing of the 295 K structure is shown on the left of Figure 1. The compound contains the "paddlewheel" $Zn_2(O_2CR)_4$ SBU core with two five-coordinate zinc(II) centers bridged equatorially by four $\mu-\kappa^2$ carboxylate ligands. The remaining axial site on each zinc atom is occupied by a dimethylsulfoxide (DMSO) molecule, which is disordered over two positions. The structure is bisected by a 2-fold rotational axis oriented horizontally and a mirror plane oriented vertically relative to the figure. The rigid phenylene groups of the ligand are oriented in the four directions implanted by the "square" SBU core and are nearly in the same plane as the carboxylate functional group. The naphthalimide rings continue this linear, square arrangement and are rotated at an average angle of 105.5° to the phenylene rings, placing them nearly perpendicular to the Zn···Zn axis.

The dimeric SBU units are organized into an open three-dimensional supramolecular network by two different types of $\pi\cdots\pi$ stacking interactions of the naphthalimide groups. These $\pi\cdots\pi$ stacking interactions are formed between naphthalimide rings of one dimer interacting with four adjacent dimeric units, Figure 2a. The first type of $\pi\cdots\pi$ stacking (A) is formed between rings colored the same, both the two light blue colored and the two dark blue colored rings. The second π-stacking interaction (B) is formed between a light blue and a dark blue ring. Both of the $\pi\cdots\pi$ stacking interactions are strong; the naphthalimide rings are 3.60 Å (A) and 3.49 Å (B) apart, and the rings are nearly parallel. Given the square arrangement of the dimers, the dipole vectors (running through the central ring carbon atoms, pointing toward the nitrogen) of the naphthalimide units involved in the $\pi\cdots\pi$ stacking interactions are

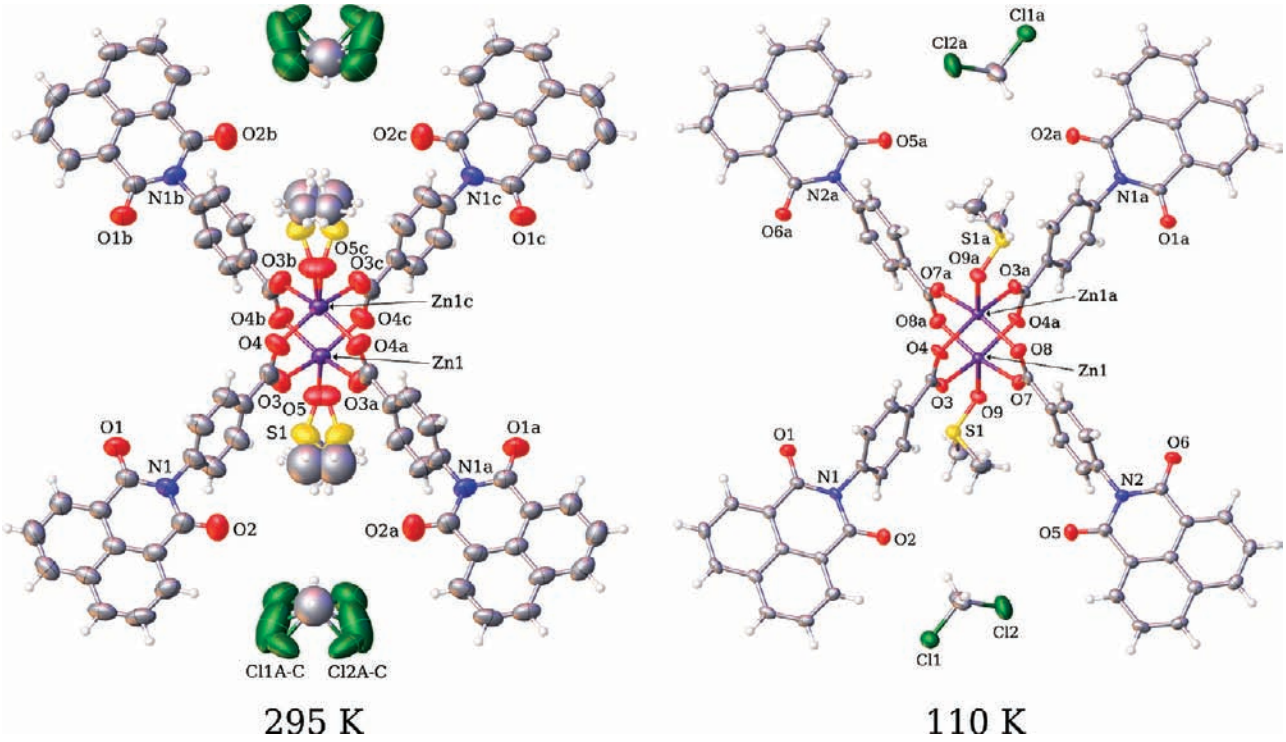

Figure 1. Molecular structures of the 295 and 110 K phases of $[Zn_2(\mathbf{L_{C4}})_4(DMSO)_2]\cdot 2(CH_2Cl_2)$. Displacement ellipsoids drawn at the 60% probability level (both). All disordered components of the 295 K structure are shown. Atom label suffixes a, b, and c denote symmetry-equivalent atoms with symmetry codes: 295 K, a = 1 −*x*, *y*, *z*; b = *x*, −*y*, 1 − *z*; c = 1 − *x*, 1 − *y*, 1 − *z*. 110 K, a = 2 − *x*, 1 − *y*, 2 − *z*.

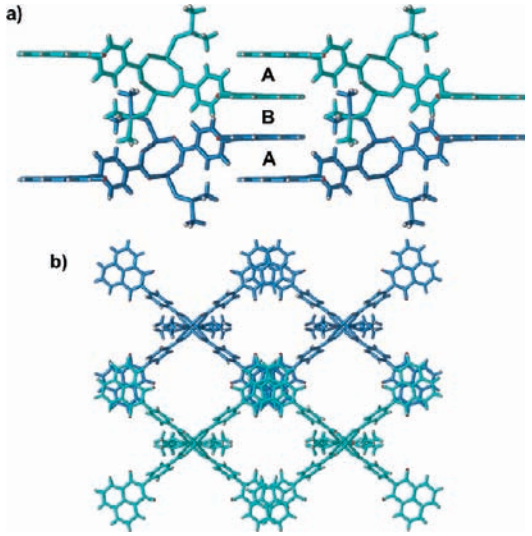

Figure 2. (a) Two pairs of stacked dimers in $[Zn_2(\mathbf{L_{C4}})_4(DMSO)_2]\cdot 2(CH_2Cl_2)$ (295 K) generating a three-dimensional network; (b) The same dimers are shown as in Figure 2a but rotated 90°.

oriented close to right angles, at 97° and 78°, respectively. An additional parameter of interest in these systems is χ, which measures the amount of slippage one ring involved in the $\pi\cdots\pi$ stack has with respect to the other. The parameter is the third side of the right triangle formed with the average perpendicular distance between the rings and the line joining the central carbon atoms of the two rings.[11d] In the room temperature structure of $[Zn_2(\mathbf{L_{C4}})_4(DMSO)_2]\cdot 2(CH_2Cl_2)$, the slippage values for the naphthalimide rings in the two interactions are 1.49 Å (A) and 0.47 Å (B), values in the range of strong interactions (0.25−2.4 Å), as previously reported.[11] Along the *c* crystallographic axis, the dimers are assembled in an ABA fashion into a three-dimensional network by the two types of $\pi\cdots\pi$ stacking interactions taking place for each of the four naphthalimide groups in each dimer. Figure 2b shows the same dimers as Figure 2a but rotated 90°, illustrating the open three-dimensional network structure of the compound.

In the overall structure of $[Zn_2(\mathbf{L_{C4}})_4(DMSO)_2]\cdot 2(CH_2Cl_2)$, there are two symmetry equivalent networks of this type, which interpenetrate generating a three-dimensional, 2-fold interpenetrated architecture. Figure 3 illustrates the blue-colored network shown in Figure 2b interpenetrated with the second purple-colored network. There are no important interactions between the two networks.

The disordered dichloromethane solvent molecules are also shown in Figure 3 and colored green. Due to the interpenetration of the two networks, they are encapsulated into the cavity created by the long rigid phenylene arms of the carboxylate ligands situated on neighboring dimers. Figure 4 pictures the third dimension (along crystallographic axis *c* direction) of the architecture illustrating the same eight dimers as Figure 3 but rotated 90° and is the same orientation as shown in Figure 2a.

Upon cooling, single crystals of $[Zn_2(\mathbf{L_{C4}})_4(DMSO)_2]\cdot 2(CH_2Cl_2)$ undergo two distinct crystallographic phase transitions, as characterized by X-ray diffraction at different temperatures. A numbered drawing of the 110 K structure is shown on the right side of Figure 1 (these numbers also apply to the 250 K structure), and selected bond lengths and angles for all three phases are gathered in Table S1 (Supporting Information). The molecular and supramolecular structures of all three phases are broadly similar, showing the 2-fold interpenetrated architecture outlined above, except for important differences noted below.

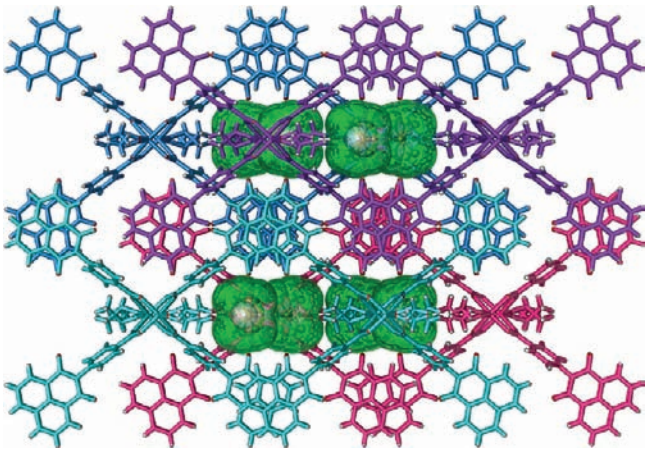

Figure 3. Three-dimensional interpenetrated network structure of $[Zn_2(\mathbf{L_{C4}})_4(DMSO)_2]\cdot 2(CH_2Cl_2)$ (295 K). The blue and purple colors delineate each network; the light and dark colors indicate eight dimers within each network. The dichloromethane solvent molecules are colored green, with all three disorder components shown.

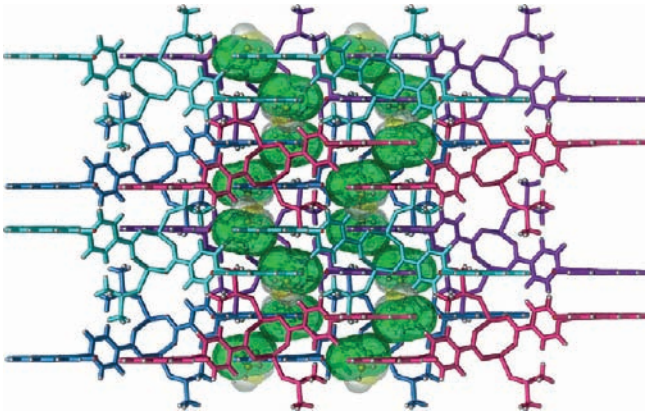

Figure 4. Third dimension of the supramolecular architecture of $[Zn_2(\mathbf{L_{C4}})_4(DMSO)_2]\cdot 2(CH_2Cl_2)$ (295 K). The same dimers are shown as in Figure 3 but rotated 90° (along crystallographic *c* axis).

The phase transitions are characterized by progressive loss of symmetry through the space groups *Cmca* → *C*2/*c* → $P2_1/n$, and twinning and ordering of coordinated DMSO molecules and uncoordinated CH_2Cl_2 guest molecules. The structural transitions occur at 265 and 195 K and are fully reversible over a number of warming-cooling cycles. The crystallographic group−subgroup relationships of the three phases can be represented by the series *Cmca* → *C*2/*c* (*t*2) → $P2_1/n$ (*k*2), where *t*2 indicates a *translationengleiche* subgroup of index 2, and *k*2 a *klassengleiche* subgroup of index 2.[16] The presence of the *translationengleiche* subgroup relationship of the first step requires the crystal to segregate into a number of domains equal to the index (two), with twinning occurring via a lost symmetry element. In this case, the twin element is a 2-fold axis along the monoclinic *a* axis and the twin pairs are related by nonmerohedry. The twinning by a 2-fold axis persists through the second *klassengleiche* phase change step, although now the diffraction patterns from the two domains are superimposed. In the first phase transition from *Cmca* → *C*2/c, the lattice translations (cell edge lengths) are essentially unchanged but there is distortion of the orthorhombic β angle from 90° to 92.769(2)°. This distortion is accompanied by a shift along the orthorhombic *a* axis direction of the $[Zn_2(\mathbf{L_{C4}})_4(DMSO)_2]$ molecules, generating $\pi\cdots\pi$ stacks that are tilted by 2.7° relative to the orthorhombic form. The shift is manifested by a change within the $\pi\cdots\pi$ stacking interactions (Table 3), causing a third type of $\pi\cdots\pi$ stacking (C); see Figure 5. This new C-type π-stacking interaction is formed between a light green and a dark green ring that was a B-type interaction at higher temperatures but now has different metric parameters. Thus, in the second phase, the dimers are held together in ABAC fashion along the *c* crystallographic axis. The most important change that results from this lowering of the symmetry is a larger χ "slippage" value of 0.87 Å in the B interaction and smaller value of 0.15 Å in the C interaction at 250 K compared to the equivalent χ value of the B interaction of 0.47 Å for the 295 K structure. This lateral shift translates through the crystal to produce a nonorthogonal axial system, i.e., a reduction in crystal symmetry from orthorhombic to monoclinic. This change is illustrated in Figure S2 (Supporting Information). Partial ordering of the DMSO and CH_2Cl_2 molecules also occurs. The DMSO molecules show 0.50/0.50 disorder occupancy at 295 K compared to 0.64/0.36 at 250 K, and the CH_2Cl_2 molecules were modeled with occupancies of 0.5/0.25/0.25 at 295 K and 0.65/0.22/0.13 at 250 K. The increase in occupancy of one component indicates nascent ordering, which becomes complete at lower temperatures. The ordering movement of these molecules likely contributes to the shift and causes the intermediate *Cmca* → *C*2/*c* phase transition, although precise analysis is obscured by the persistence of disorder. At 110 K, the DMSO and CH_2Cl_2 molecules are both fully ordered (see Figure 1). Remarkably, the lateral shift and tilting of the $\pi\cdots\pi$ stacks has disappeared, and the supramolecular structure has reverted to the 295 K form, with the critical difference being the presence of fully ordered solvent species. This similarity is apparent upon comparison of the reduced unit cell parameters for the 295 and 110 K phases; taking into account the cell contraction as a function of temperature, they are essentially the same.

The observed solvent ordering is likely driven by a reduction in thermal energy for molecular motion as well as temperature contraction of the unit cell. Disorder requires space; the DMSO and CH_2Cl_2 molecules have less available "free space" in which to adopt multiple orientations on their crystallographic sites throughout the crystal. An increasingly confined environment caused by shortening of the nonbonded distances of the host framework upon contraction induces the molecules to order. It is the ordering of the CH_2Cl_2 molecules alone which drives the symmetry-breaking phase transitions. As evident in Figure S3 (Supporting Information), the low-temperature ordered arrangement of the CH_2Cl_2 molecules in the 110 K $P2_1/n$ phase is clearly not consistent with the additional mirror and 2-fold rotational symmetry present in the orthorhombic form. The ordering of the DMSO is a response to ordering of the CH_2Cl_2 molecules, owing to the close proximity of these species in the crystal. A data set of the hydrated form collected at 110 K, which undergoes no phase change (space group *Cmca* from 296 to 110 K) showed that the DMSO species remain disordered in the absence of the ordered CH_2Cl_2 (vide infra).

Single-Crystal to Single-Crystal Transformations. Crystals of $[Zn_2(\mathbf{L_{C4}})_4(DMSO)_2]\cdot 2(CH_2Cl_2)$ were placed under vacuum for approximately 3 days, followed by mounting of the crystals for X-ray diffraction in air. The diffraction experiment showed that

Table 3. $\pi\cdots\pi$ Stacking Interaction Parameters

T (K)	interaction type	central carbon-central carbon (Å)	dipole angle (deg)	plane angle (deg)	avg. perpendicular distance (Å)	avg. slippage, χ (Å)
295	A	3.89	97	4.0	3.60	1.49
	B	3.52	78	4.0	3.49	0.47
250	A	3.86	98	2.5	3.54	1.53
	B	3.57	79	1.2	3.47	0.87
	C	3.47	75	3.5	3.46	0.15
110	A	3.79	97	3.8	3.52	1.41
	B	3.47	79	1.9	3.44	0.48

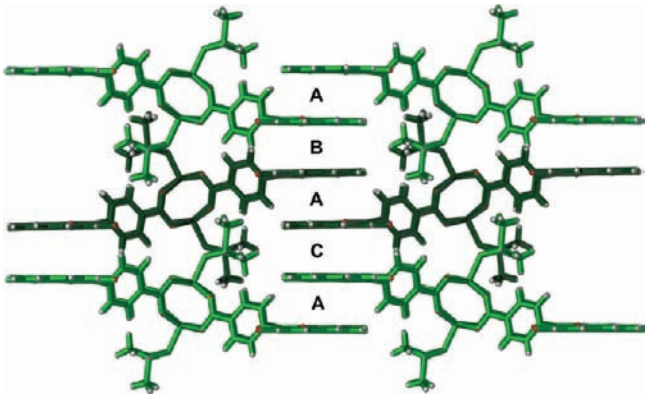

Figure 5. Naphthalimide $\pi\cdots\pi$ stacking interactions in the intermediate C-centered monoclinic phase (265−195 K) of $[Zn_2(\mathbf{L_{C4}})_4(DMSO)_2]\cdot 2(CH_2Cl_2)$ generating a three-dimensional network.

these crystals were now $[Zn_2(\mathbf{L_{C4}})_4(DMSO)_2]\cdot 2.3(H_2O)$, demonstrating a gas/solid-mediated, single-crystal to single-crystal transformation had taken place (see Figure 6). X-ray diffraction data on a number of samples demonstrates that the maximum amount of H_2O molecules/Zn_2 units that can be picked up is 3.9. The exchange of water for the methylene chloride also takes place over days on crystals of $[Zn_2(\mathbf{L_{C4}})_4(DMSO)_2]\cdot 2(CH_2Cl_2)$ left in the air.

At room temperature, the hydrated $[Zn_2(\mathbf{L_{C4}})_4(DMSO)_2]\cdot 3.9(H_2O)$ complex has the same C-centered orthorhombic structure (space group *Cmca*, unit cell volume 7156.9 Å^3) as the dichloromethane adduct at the same temperature but does not change symmetry at lower temperature. Apparently, the mobility and "compressibility" enabled by partially occupied, "small", mobile water molecules in the place of fully occupied, larger methylene chloride molecules allows the host framework enough freedom of movement to adapt to the contracting unit cell, and therefore, no symmetry-breaking crystallographic phase changes are observed. The molecular and the supramolecular structure of both forms of the hydrated complex are similar to the dichloromethane complex. Selected bond lengths and angles for both hydrated forms are gathered in Table S2 (Supporting Information). Again, two types of $\pi\cdots\pi$ stacking interactions organize the dimers into an open three-dimensional network, which is interpenetrating with a second network to generate a 2-fold interpenetrated architecture. The metrics of the two $\pi\cdots\pi$ stacking interactions are slightly different than in the dichloromethane adduct, but both interactions fall in the range of a strong naphthalimide π-stacking interaction. Table 4 contains

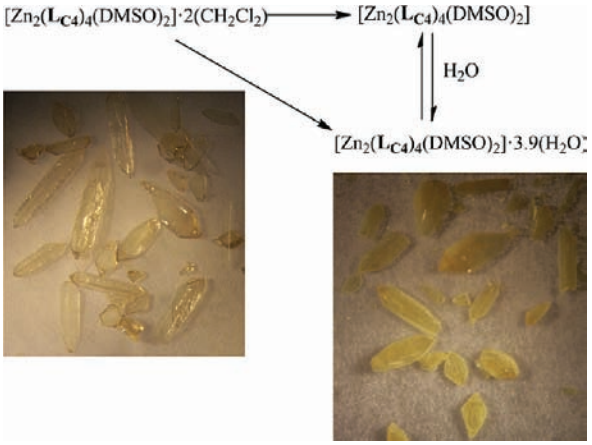

Figure 6. Single-crystal to single-crystal transformation with $[Zn_2(\mathbf{L_{C4}})_4(DMSO)_2]$ crystals. Left: picture taken on the as collected crystals of $[Zn_2(\mathbf{L_{C4}})_4(DMSO)_2]\cdot 2(CH_2Cl_2)$ from the mother liquor. Right: picture of $[Zn_2(\mathbf{L_{C4}})_4(DMSO)_2]\cdot 3.9(H_2O)$ taken after TGA cycle of heating of the $[Zn_2(\mathbf{L_{C4}})_4(DMSO)_2]\cdot 2(CH_2Cl_2)$ crystals to 100 °C in dry air followed by cooling to room temperature in ambient air (see below and Figure 10).

the $\pi\cdots\pi$ stacking interaction parameters for two hydrated species containing 2.3 and 3.9 H_2O molecules per dimeric unit.

Figure 7 illustrates the $[Zn_2(\mathbf{L_{C4}})_4(DMSO)_2]$ frameworks with the two different guests. In the case of $[Zn_2(\mathbf{L_{C4}})_4(DMSO)_2]\cdot 2(CH_2Cl_2)$ (Figure 7, left), the solvent molecules are mainly "trapped" in the lattice, although there are weak C−H···Cl interactions with a CH···Cl distance of 2.96 Å (C···Cl = 3.87 Å) and a CHCl angle of 168° between the dichloromethane guest and the naphthalimide rings of the framework. In the case of the hydrated compound (Figure 7, right), the guest molecules are bonded to the framework by stronger (magenta dots) and weaker (green dots) C−H···O interactions. The C−H···O interactions of the guest molecules with the naphthalimide rings of the framework are strong with a CH···O distance of 2.60 Å (C···O = 3.52 Å) and CHO angle of 172°. The less favorable C−H···O interactions are formed between the guest molecules and the dimethylsulfoxide axial ligands with a CH···O distance of 2.79 Å (C···O = 3.35 Å) and CHO angle of 118°.

It is worth noting that although both frameworks contain pockets of solvent, none of the compounds or phases possess permanent porosity. Figure 8 pictures two units of the $[Zn_2(\mathbf{L_{C4}})_4(DMSO)_2]\cdot 3.9(H_2O)$ framework shown in Figure 7 (right) but rotated 90° in the horizontal direction. Additionally, two units (purple colored) of the interpenetrating second network are shown. It can be noticed that the water molecules are encapsulated into the cavity created by the four interpenetrating dimeric units. The cavity measures approximately 15.7 Å × 3.7 Å. The remarkable feature of the single-crystal to single-crystal transformation is that, even though neither of the two compounds are porous solids, the methylene chloride is easily removed and the water can permeate into the cavity without the loss of crystallinity.

The presence of the H_2O in the crystal structure was also demonstrated by infrared spectroscopy. Figure S4 (Supporting Information) shows the IR spectra of the dichloromethane and the water solvated species. The broad O−H stretching band at 3474 cm^{-1} corresponds to the solvent of crystallization in the

dx.doi.org/10.1021/ic201830h |*Inorg. Chem.* 2011, 50, 11754–11764

Table 4. $[Zn_2(L_{C4})_4(DMSO)_2]\cdot n(H_2O)$ $\pi\cdots\pi$ Stacking Interaction Parameters

nH_2O	interaction type	central carbon-central carbon (Å)	dipole angle (deg)	plane angle (deg)	avg. perpendicular distance (Å)	avg. slippage, χ (Å)
2.3	A	3.73	94	1.8	3.49	1.32
	B	3.46	82	4.9	3.42	0.50
3.9	A	3.72	93	1.1	3.48	1.32
	B	3.44	82	5.1	3.41	0.46

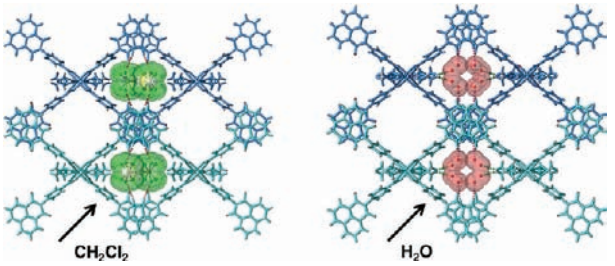

Figure 7. $[Zn_2(L_{C4})_4(DMSO)_2]$ framework with guests CH_2Cl_2 (left) and H_2O (right). The C—H···Cl and stronger C—H···O interactions are represented by magenta dots, and the weaker C—H···O interactions are represented by green dots.

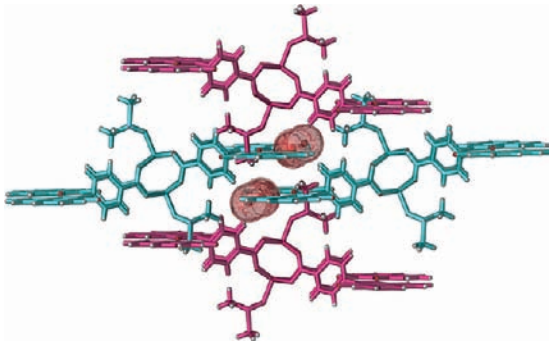

Figure 8. Encapsulated H_2O guest molecules in the cavity of the $[Zn_2(L_{C4})_4(DMSO)_2]\cdot 3.9(H_2O)$ framework.

$[Zn_2(L_{C4})_4(DMSO)_2]\cdot 3.9(H_2O)$ framework (see bottom spectrum, Figure S4, Supporting Information). The spectra from 400 to 2000 cm^{-1} are remarkably similar.

Thermogravimetric Analysis. TGA analysis of the $[Zn_2(L_{C4})_4(DMSO)_2]\cdot 2.3(H_2O)$ crystals (see Figure 9) also corroborates the presence of 2.3 water molecules/Zn_2 unit in the crystal of the sample used in the first structural study. Upon heating, the weight loss of 3.1% (calcd. 2.6%) in the first step corresponds to the loss of the 2.3 water molecules of crystallization. In the next step, between 161 and 330 °C, the loss of the two coordinated dimethylsulfoxide molecules occurs (10.4%, calcd: 9.8%). The weight change in the last step corresponds to the loss of the four carboxylate ligands (77.9%, calcd: 77.4%). The final residual weight is 8.5% corresponding to ZnO (calcd: 10.2%).

The single-crystal to single-crystal transformations can also be followed by TGA. A crystalline sample of $[Zn_2(L_{C4})_4(DMSO)_2]\cdot 2(CH_2Cl_2)$ was heated to 100 °C and held at that temperature for 15 min; this sample lost the weight expected for the removal of two

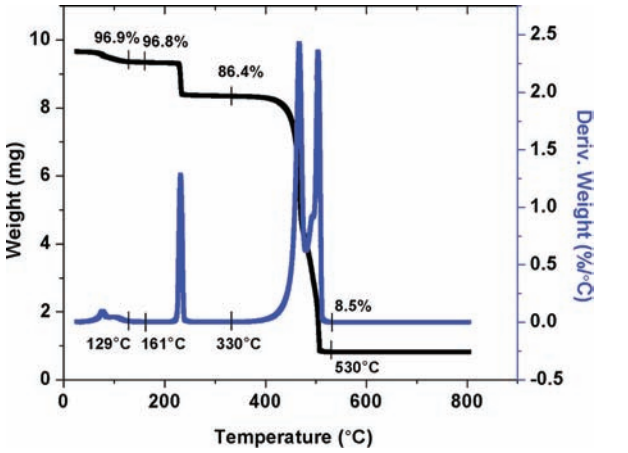

Figure 9. TGA and DTA curves for $[Zn_2(L_{C4})_4(DMSO)_2]\cdot 2.3(H_2O)$.

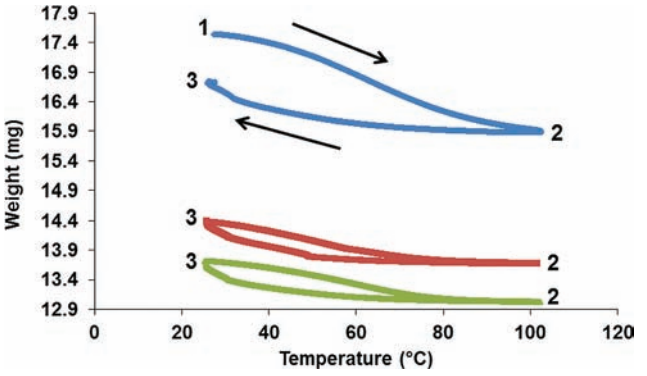

Figure 10. Controlled TGA of crystalline samples of $[Zn_2(L_{C4})_4(DMSO)_2]\cdot 2(CH_2Cl_2)$ (**1**) and $[Zn_2(L_{C4})_4(DMSO)_2]\cdot 3.9(H_2O)$ (**3**). Top: TGA of sample of $[Zn_2(L_{C4})_4(DMSO)_2]\cdot 2(CH_2Cl_2)$ (**1**) to form $[Zn_2(L_{C4})_4(DMSO)_2]$ (**2**) at 100 °C followed by cooling in ambient air to form $[Zn_2(L_{C4})_4(DMSO)_2]\cdot 3.9(H_2O)$ (**3**). Middle and bottom: Two cycles of dehydration and rehydration of $[Zn_2(L_{C4})_4(DMSO)_2]\cdot 3.9(H_2O)$. Part of the sample was removed for X-ray analysis after each run, thus changing the starting weight of each cycle.

CH_2Cl_2 molecules (calcd: 9.86%, found: 9.38%) forming unsolvated $[Zn_2(L_{C4})_4(DMSO)_2]$. The sample was then cooled and left in the ambient air of the TGA chamber, during which time a weight gain corresponding to the expected 3.9 mol H_2O/Zn_2 unit was observed (calcd: 4.33%, found: 4.71%), Figure 10 (top curve). Importantly, the sample is still crystalline and its constitution as $[Zn_2(L_{C4})_4(DMSO)_2]\cdot 3.9(H_2O)$ was verified by single-crystal X-ray crystallography. Moreover, these hydrated crystals can be dehydrated and rehydrated in a reversible process in which the sample retains crystallinity. As shown in the middle of Figure 10, heating the sample of the now $[Zn_2(L_{C4})_4(DMSO)_2]\cdot 3.9(H_2O)$ (removal of crystals for the X-ray experiment causes a weight loss between the first and second experiments) to 100 °C reforms $[Zn_2(L_{C4})_4(DMSO)_2]$ and cooling as in the first experiment leads to the reformation of $[Zn_2(L_{C4})_4(DMSO)_2]\cdot 3.9(H_2O)$ (calcd: 4.33%, found: 4.90%). As shown in the bottom of Figure 10, this same sequence was repeated again (again less sample was present in the final run due to removal of crystals for X-ray analysis). As in the first step, the crystals maintain their crystallinity during this process as demonstrated by single-crystal

dx.doi.org/10.1021/ic201830h |*Inorg. Chem.* 2011, 50, 11754–11764

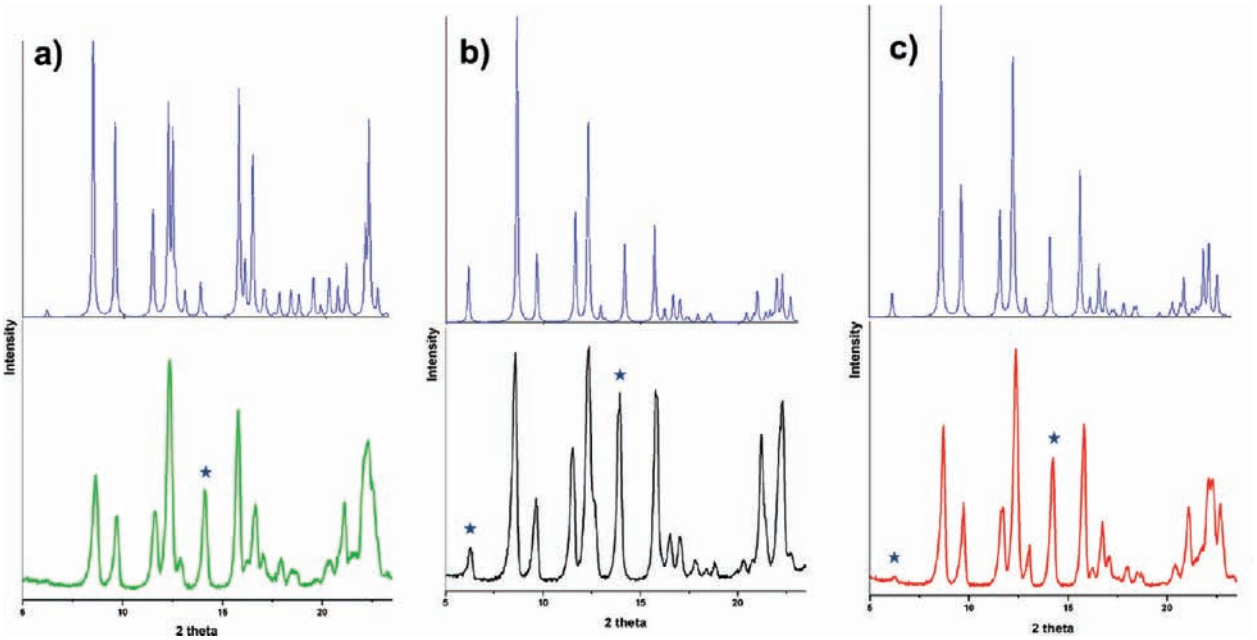

Figure 11. Simulated (top) and measured (bottom) powder X-ray diffraction of (a) $[Zn_2(\mathbf{L_{C4}})_4(DMSO)_2]\cdot 2(CH_2Cl_2)$, (b) $[Zn_2(\mathbf{L_{C4}})_4(DMSO)_2]$, and (c) $[Zn_2(\mathbf{L_{C4}})_4(DMSO)_2]\cdot 3.9(H_2O)$.

X-ray diffraction performed after each cycle (see Figure 6). These experiments demonstrate the exceptional thermal stability of the $[Zn_2(\mathbf{L_{C4}})_4(DMSO)_2]$ framework and also represent an unusual example of a gas/solid single-crystal to single-crystal transformation followed by TGA.

Powder X-ray Analysis. The above TGA experiments were supported by powder X-ray diffraction studies carried out under analogous conditions. The powder X-ray diffraction of a ground sample of $[Zn_2(\mathbf{L_{C4}})_4(DMSO)_2]\cdot 2(CH_2Cl_2)$ (**1**) matches the spectrum predicted from the single-crystal experiments, Figure 11a. This sample was heated in a nitrogen atmosphere to 100 °C, and the powder X-ray pattern matches that predicted for $[Zn_2(\mathbf{L_{C4}})_4(DMSO)_2]$ (**2**), using the structure of **1** as the model with removal of the methylene chloride solvates. Clearly, crystallinity has been maintained for this sample that now contains no solvent of crystallization, and the spectrum has changed versus that observed for **1**. The spectrum looks the same after this sample was cooled under nitrogen to ambient temperature. The sample was then allowed to sit in ambient air for 48 h, and the spectrum was recorded again, showing a new pattern that matches that predicted for $[Zn_2(\mathbf{L_{C4}})_4(DMSO)_2]\cdot 3.9(H_2O)$ (**3**) from the single-crystal work. In comparing the three spectra, which have a similar overall appearance, as expected, given the similarity of the samples that are all in the space group *Cmca*, the most notable change is the peak at 2θ = 6.3° that is very apparent in the "empty" framework but only just noticeable in the water solvate and not present at all in the methylene chloride sample. The peak at 2θ = 13.8° also noticeably changes intensity along this series.

UV−vis and Fluorescence Spectral Properties of $[Zn_2(L_{C4})_4(DMSO)_2]\cdot 2(CH_2Cl_2)$ and $[Zn_2(L_{C4})_4(DMSO)_2]\cdot 3.9(H_2O)$. The diffuse reflectance (UV−vis) spectra of the protonated form of the ligand, $H\mathbf{L_{C4}}$, and the two complexes, $[Zn_2(\mathbf{L_{C4}})_4(DMSO)_2]\cdot 2(CH_2Cl_2)$ and $[Zn_2(\mathbf{L_{C4}})_4(DMSO)_2]\cdot 3.9(H_2O)$, show a sharp maxima, $\lambda_{max,UV}$, at 365 nm for $H\mathbf{L_{C4}}$, and a broader band centered approximately at 384 nm for the two complexes. The fluorescence emission profile of the compounds was also recorded in the solid state at room temperature (Figure 12). $H\mathbf{L_{C4}}$ shows blue fluorescence with a $\lambda_{max,Fl}$ at 441 nm. For the two complexes, $\lambda_{max,Fl}$ was at 475 and 484 nm, which were significantly red-shifted compared to the free ligand.

DISCUSSION

A novel zinc-based supramolecular metal−organic framework solid (SMOF), $[Zn_2(\mathbf{L_{C4}})_4(DMSO)_2]\cdot 2(CH_2Cl_2)$, which combines the robust $Zn_2(O_2CR)_4$ SBU core with the $\pi\cdots\pi$ stacking capabilities of the 1,8-naphthalimide supramolecular synthon, was prepared and characterized. As expected from the design of the $\mathbf{L_{C4}}^-$ ligand, which has a long, linear link between the two functional groups, the "square" architecture of the SBU core is retained in the molecular structure. As shown in Figure 2b, the linear directional orientation of the phenylene arms places the naphthalimide rings of adjacent dimers in positions where they can form $\pi\cdots\pi$ stacking interactions in which the dipole vectors of the rings are oriented at nearly right angles, leading to the formation of a three-dimensional open framework. The accessible region in this open network is occupied by interpenetration of a second three-dimensional network structure (Figure 3) and two dichloromethane solvates of crystallization. This unique 2-fold interpenetrated three-dimensional architecture is organized solely by noncovalent $\pi\cdots\pi$ stacking interactions.

Incorporating a bifunctional carboxylate ligand bearing the strong 1,8-naphthalimide π-stacking synthon into the $Zn_2(O_2CR)_4$ SBU core leads to a material with novel properties as well as interesting structural characteristics. Single crystals of the $[Zn_2(\mathbf{L_{C4}})_4(DMSO)_2]\cdot 2(CH_2Cl_2)$ complex undergo two successive symmetry-breaking crystallographic phase changes upon lowering the temperature, resulting in three distinct but very similar structures. The compound retains crystallinity after each phase change, adopting space groups *Cmca* (T > 265 K), *C*2/*c* (265−195 K) and $P2_1/n$ (T < 195 K), and was thoroughly

dx.doi.org/10.1021/ic201830h |*Inorg. Chem.* 2011, 50, 11754–11764

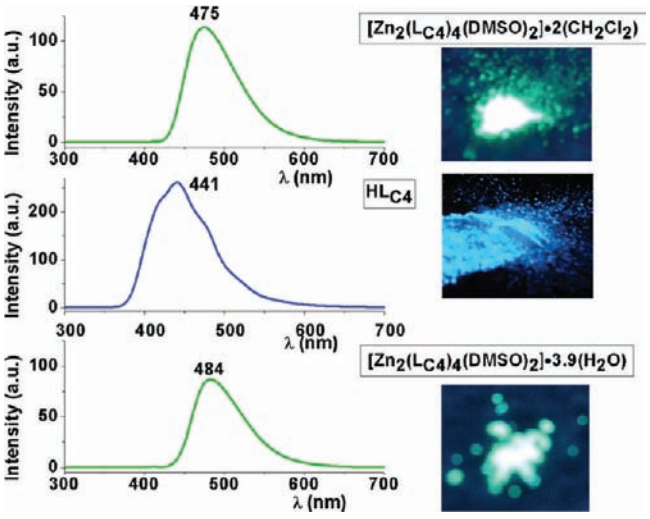

Figure 12. Fluorescence emission spectra of HL_{C4} (excitation at 263 nm), $[Zn_2(\mathbf{L_{C4}})_4(DMSO)_2]\cdot 2(CH_2Cl_2)$ (excitation at 412 nm), and $[Zn_2(\mathbf{L_{C4}})_4(DMSO)_2]\cdot 3.9(H_2O)$ (excitation at 413 nm) in the solid state. Excitation of the complexes at 263 and 380 nm resulted in the same emission profile.

characterized by single-crystal X-ray diffraction at each step. The phase changes are reversible and are clearly driven by thermally induced ordering (cooling) or disordering (warming) of dichloromethane guest molecules. The absence of such phase changes in the CH_2Cl_2-free, hydrated forms of the compound is strong support for the critical role of the CH_2Cl_2 molecules. Order/disorder type phase transitions have been previously observed in inorganic−organic hybrid materials, and in several cases, practical applications of these materials have been reported.[17] Occurrences of multiple phase transitions studied by X-ray diffraction in the same single crystal are rare.[18]

A second interesting property of these solids is that crystals of $[Zn_2(\mathbf{L_{C4}})_4(DMSO)_2]\cdot 2(CH_2Cl_2)$ undergo a single-crystal to single-crystal gas/solid guest exchange upon exposure to atmospheric moisture or faster if placed under vacuum or heated to 100 °C under a dry gas before being shown atmospheric moisture, yielding $[Zn_2(\mathbf{L_{C4}})_4(DMSO)_2]\cdot 3.9(H_2O)$. This new compound possesses the same three-dimensional interpenetrated framework structure (no change in space group) as the dichloromethane adduct. The water molecules are encapsulated into the same cavities where the dichloromethane molecules were residing, although they have stronger noncovalent interactions with the network. The solvate free intermediate, $[Zn_2(\mathbf{L_{C4}})_4(DMSO)_2]$, was characterized by TGA and powder X-ray diffraction studies and also holds the structure observed for the dichloromethane and water adducts at 100 °C, the high temperature limit measured in these studies. Importantly, even though the cavities that hold the solvates are created by the long rigid arms of the ligands, these compounds do not possess channel like void spaces which would classify them as porous solids. The remarkable feature of the single-crystal to single-crystal guest exchange is that, even though the frameworks are not porous, the relatively large methylene chloride guest molecules can readily "leave" the solid and water guest molecules can permeate back into the cavities without the loss of crystallinity and with no phase change.

By organizing the solids reported here with strong and flexible $\pi\cdots\pi$ stacking interactions, the compounds possess a robust but dynamic supramolecular network that retains integrity and crystallinity upon removal and uptake of "guest" solvent molecules. This unique framework also enables the cooperative reorganization necessary for the two phase transitions observed by changing the temperature of the CH_2Cl_2 adduct without loss of crystalline integrity. Importantly, comparisons of the crystal structures of the different solvates and three phases of $[Zn_2(\mathbf{L_{C4}})_4(DMSO)_2]\cdot 2(CH_2Cl_2)$ allow the direct observation of changes in the $\pi\cdots\pi$ stacking interactions (see Tables 3 and 4), changes that show the local flexibility built into these solids by design. Thus, by combining strong but flexible noncovalent interactions with the classic SBU central core of the $Zn_2(O_2CR)_4$ unit, the resulting SMOF solids that are obtained are robust enough to maintain overall structure but have local flexibility to permit guest transport in a nonporous material and phase changes without loss of crystallinity.

Also, the presence of the naphthalimide rings in both CH_2Cl_2 and H_2O solvates leads to green emission in the solid state that can likely be assigned to a charge transfer transition. In addition to the green luminescence, the exceptional thermal stability of these complexes, as well as the fact that they are insoluble in common organic solvents, makes them a good candidate for use as green-fluorescent materials.[9a,19]

CONCLUSION

We have shown that judicious ligand design can lead to novel materials with interesting properties. The above structural studies coupled with our earlier work[11] demonstrate that the 1,8-naphthalimide group is a reliable supramolecular synthon that can be transferred from one system to another to generate high-dimensionality materials. Importantly, the $\pi\cdots\pi$ stacking interactions of the naphthalimide rings allow the formation of "robust" frameworks (SMOFs) that have "local flexibility". The flexible but robust $\pi\cdots\pi$ stacking interaction of the naphthalimide rings facilitates temperature induced phase changes and the exchange of small guest molecules without the loss of crystallinity. As shown in Tables 3 and 4, the metrics of the naphthalimide π-stacking interactions are changing somewhat in the different crystalline phases and solvates, but the overall strength of these interactions does not change to any appreciable degree. The naphthalimide ring interactions allow a slight "dynamic motion" of the frameworks to permit phase changes and the exchange of new guest molecules without the loss of crystallinity. Similar single-crystal to single-crystal gas/solid-mediated transformations have also been observed previously in homochiral metal complexes organized in one dimension by $\pi\cdots\pi$ stacking interactions of 1,8-naphthalimide rings. In these cases, water molecules that were trapped in pockets in the densely packed structures could be readily removed and reintroduced.[11g,h] Thus, we have used crystal engineering for the rational design of robust network solids with local flexibility that show single-crystal to single-crystal phase changes and gas/solid guest exchange transformations.[8,9,20]

ASSOCIATED CONTENT

Supporting Information. X-ray crystallographic files in CIF format for the structural determinations, figures of evolution of diffraction peak profiles, comparisons 295, 250, and 110 K unit cells of $[Zn_2(\mathbf{L_{C4}})_4(DMSO)_2]\cdot 2(CH_2Cl_2)$, selected bond

distances and angles, and infrared spectra. This material is available free of charge via the Internet at http://pubs.acs.org.

AUTHOR INFORMATION

Corresponding Author
*E-mail: Reger@chem.sc.edu.

ACKNOWLEDGMENT

The authors acknowledge with thanks the financial support of the National Science Foundation through grant CHE-1011736. The authors would also like to thank Dr. Daniel E. Bugaris for running the powder XRD and the reviewers for thoughtful comments.

REFERENCES

(1) (a) Phan, A.; Czaja, A. U.; Gandara, F.; Knobler, C. B.; Yaghi, O. M. *Inorg. Chem.* **2011**, *50*, 7388. (b) Dhakshinamoorthy, A.; Alvaro, M.; Corma, A.; Garcia, H. *Dalton Trans.* **2011**, *40*, 6344. (c) Corma, A.; Garcia, H.; Llabrés i Xamena, F. X. *Chem. Rev.* **2010**, *110*, 4606, and references therein. (d) Farrusseng, D.; Aguado, S.; Pinel, C. *Angew. Chem., Int. Ed.* **2009**, *48*, 7502. (e) Tanabe, K. K.; Cohen, S. M. *Inorg. Chem.* **2010**, *49*, 6766. (f) Lin, W. *Top. Catal.* **2010**, *53*, 869. (g) Wu, C.-D.; Hu, A.; Zhang, L.; Lin, W. *J. Am. Chem. Soc.* **2005**, *127*, 8941. (h) Qiu, S.; Zhu, G. *Coord. Chem. Rev.* **2009**, *253*, 2891.

(2) (a) Murray, L. J.; Dinca, M.; Long, J. R. *Chem. Soc. Rev.* **2009**, *38*, 1294. (b) Czaja, A. U.; Trukhan, N.; Muller, U. *Chem. Soc. Rev.* **2009**, *38*, 1284. (c) Muller, U.; Schubert, M.; Teich, F.; Puetter, H.; Schierle-Arndt, K.; Pastre, J. *J. Mater. Chem.* **2006**, *38*, 626. (d) Rowsell, J. C. L.; Spencer, E. C.; Eckert, J.; Howard, J. K.; Yaghi, O. M. *Science* **2005**, *309*, 1350. (e) Morris, R. E.; Wheatley, P. S. *Angew. Chem., Int. Ed.* **2008**, *47*, 4966. (f) Rowsell, J. L. C.; Yaghi, O. M. *Angew. Chem., Int. Ed.* **2005**, *44*, 4670. (g) Matsuda, R.; Kitaura, R.; Kitagawa, S.; Kubota, Y.; Belosludov, R. V.; Kobayashi, T. C.; Sakamoto, H.; Chiba, T.; Takata, M.; Kawazoe, Y.; Mita, Y. *Nature* **2005**, *436*, 238. (h) Millward, A. R.; Yaghi, O. M. *J. Am. Chem. Soc.* **2005**, *127*, 17998. (i) Ro, J. C.; Eckert, J.; Yaghi, O. M. *J. Am. Chem. Soc.* **2005**, *127*, 14904. (j) Li, Y.; Yang, R. T. *Langmuir* **2007**, *23*, 12937.

(3) (a) Chen, B.; Xiang, S.; Qian, G. *Acc. Chem. Res.* **2010**, *43*, 1115. (b) Liu, S.; Li, J.; Luo, F. *Inorg. Chem. Commun.* **2010**, *13*, 870. (c) Green, M. A. *Nat. Mater.* **2010**, *9*, 539. (d) Lan, A.; Li, K.; Wu, H.; Olson, D.; Emge, T.; Ki, W.; Hong, M.; Li, J. *Angew. Chem., Int. Ed.* **2009**, *48*, 2334. (e) Chen, B.; Yang, Y.; Zapata, F.; Lin, G.; Qian, G.; Lobkovsky, E. B. *Adv. Mater.* **2007**, *19*, 1693.

(4) (a) Czaja, A. U.; Trukhan, N.; Muller, U. *Chem. Soc. Rev.* **2009**, *38*, 1284, and references therein. (b) Qiu, S.; Zhu, G. *Coord. Chem. Rev.* **2009**, *253*, 2891. (c) Manos, M. J.; Iyer, R. G.; Quarez, E.; Liao, J. H.; Kanatzidis, M. G. *Angew. Chem., Int. Ed.* **2005**, *44*, 3552. (d) Lee, H.; Zones, S. I.; Davis, M. E. *Nature* **2003**, *425*, 385. (e) Corma, A. *Chem. Rev.* **1997**, *97*, 2373, and references therein.

(5) (a) Tranchemontagne, D. J.; Mendoza-Cortes, J. L.; O'Keeffe, M.; Yaghi, O. M. *Chem. Soc. Rev.* **2009**, *38*, 1257. (b) Rao, C. N. R.; Natarajan, S.; Vaidhyanathan, R. *Angew. Chem., Int. Ed.* **2004**, *43*, 1466. (c) Yaghi, O. M.; O'Keeffe, M.; Ockwig, N. W.; Chae, H. K.; Eddaoudi, M.; Kim, J. *Nature* **2003**, *423*, 705. (d) Eddaoudi, M.; Moler, D. B.; Li, H.; Chen, B.; Reineke, T. M.; O'Keeffe, M.; Yaghi, O. M. *Acc. Chem. Res.* **2001**, *34*, 319. (e) Biradha, K.; Ramanan, A.; Vittal, J. J. *Cryst. Growth Des.* **2009**, *9*, 2969.

(6) (a) Perry, J. J., IV; Perman, J. A.; Zaworotko, M. J. *Chem. Soc. Rev.* **2009**, *38*, 1400. (b) Robson, R. *J. Chem. Soc., Dalton Trans.* **2008**, 5113. (c) Moulton, B.; Zaworotko, M. J. *Chem. Rev.* **2001**, *101*, 1629. (d) Yong, G.-P.; Wang, Z.-Y.; Cui, Y. *Eur. J. Inorg. Chem.* **2004**, 4317. (e) Evans, O. R.; Wang, Z.; Xiong, R.-G.; Foxman, B. M.; Lin, W. *Inorg. Chem.* **1999**, *38*, 2969.

(7) (a) Steed, J. W.; Atwood, J. L. *Supramolecular Chemistry*, 2nd ed.; John Wiley & Sons, Ltd, Oxford, U.K., 2009; pp 28−32. (b) Braga, D.; Brammer, L.; Champness, N. R. *CrystEngComm* **2005**, *7*, 1. (c) Moulton, B.; Zaworotko, M. J. *Chem. Rev.* **2001**, *101*, 1629.

(8) (a) Horike, S.; Shimomura, S.; Kitagawa, S. *Nature Chem.* **2009**, *1*, 695. (b) Fujita, M.; Kawano, M. *Coord. Chem. Rev.* **2007**, *251*, 2592. (c) Uemura, K.; Saito, K.; Kitagawa, S.; Kita, H. *J. Am. Chem. Soc.* **2006**, *128*, 16122. (d) Kitagawa, S.; Uemura, K. *Chem. Soc. Rev.* **2005**, *34*, 109. (e) Kitagawa, S.; Kitaura, R.; Noro, S. *Angew. Chem., Int. Ed.* **2004**, *43*, 2334. (f) Uemura, K.; Kitagawa, S.; Kondo, M.; Fukui, K.; Kitaura, R.; Chang, H.-C.; Mizutani, T. *Chem.—Eur. J.* **2002**, *8*, 3587. (g) Jiang, J.-J.; Li, L.; Lan, M.-H.; Pan, M.; Eichhofer, A.; Fenske, D.; Su, C.-Y. *Chem.—Eur. J.* **2010**, *16*, 1841.

(9) (a) Guo, H.; Guo, X.; Batten, S. R.; Song, J.; Song, S.; Dang, S.; Zheng, G.; Tang, J.; Zhang, H. *Cryst. Growth Des.* **2009**, *9*, 1394. (b) Hu, S.; He, K.-H.; Zeng, M.-H.; Zou, H.-H.; Jiang, Y.-M. *Inorg. Chem.* **2008**, *47*, 5218.

(10) (a) Janiak, C. *J. Chem. Soc., Dalton Trans.* **2000**, 3885. (b) Hunter, C. A.; Sanders, J. K. M. *J. Am. Chem. Soc.* **1990**, *112*, 5525. (c) Steed, J. W.; Atwood, J. L. *Supramolecular Chemistry*, 2nd ed.; John Wiley & Sons, Ltd, Oxford, U.K., 2009; pp 33−35.

(11) (a) Reger, D. L.; Elgin, J. D.; Semeniuc, R. F.; Pellechia, P. J.; Smith, M. D. *Chem. Commun.* **2005**, 4068. (b) Reger, D. L.; Semeniuc, R. F.; Elgin, J. D.; Rassolov, V.; Smith, M. D. *Cryst. Growth Des.* **2006**, *6*, 2758. (c) Reger, D. L.; Elgin, J. D.; Smith, M. D; Simpson, B. K. *Polyhedron* **2009**, *28*, 1469. (d) Reger, D. L.; Debreczeni, A.; Reinecke, B.; Rassolov, V.; Smith, M. D.; Semeniuc, R. F. *Inorg. Chem.* **2009**, *48*, 8911. (e) Reger, D. L.; Debreczeni, A.; Smith, M. D. *Inorg. Chim. Acta* **2010**, *364*, 10. (f) Reger, D. L.; Horger, J.; Smith, M. D. *Chem. Commun.* **2011**, *47*, 2805. (g) Reger, D. L.; Horger, J.; Smith, M. D.; Long, G. J. *Chem. Commun.* **2009**, 6219. (h) Reger, D. L.; Horger, J. J.; Smith, M. D.; Long, G. J.; Fernande, G. *Inorg. Chem.* **2011**, *50*, 686. (i) Reger, D. L.; Debreczeni, A.; Horger, J. J.; Smith, M. D. *Cryst. Growth Des.* **2011**, *11*, 4068.

(12) *SMART Version 5.630, SAINT+ Version 6.45, SADABS Version 2.10, and TWINABS*. Bruker Analytical X-ray Systems, Inc.: Madison, Wisconsin, USA, 2003.

(13) Sheldrick, G. M. *Acta Crystallogr.* **2008**, *A64*, 112.

(14) *CELL_NOW*. Bruker AXS Inc.: Madison, Wisconsin, USA, 2005.

(15) Rowland, R. S.; Taylor, R. *J. Phys. Chem.* **1996**, *100*, 7384.

(16) *Translationgleiche* subgroup: subgroup in which the crystal class (point group) is changed but unit cell translations are the same. *Klassengleiche* subgroup: subgroup in which the unit cell translations are changed but the crystal class (point group) is retained. See Müller, U. *Inorganic Structural Chemistry*, 2nd ed.; John Wiley & Sons, Ltd: Oxford, UK, 1993, pp 235−246.

(17) (a) Jain, P.; Dalal, N. S.; Toby, B. H.; Kroto, H. W.; Cheetham, A. K. *J. Am. Chem. Soc.* **2008**, *130*, 10450. (b) Wu, H.; Zhou, W.; Yildirim, T. *J. Phys. Chem. C* **2009**, *113*, 3029. (c) Jeftic, J.; Hauser, A. *J. Phys. Chem. B* **1997**, *101*, 10262.

(18) (a) Görbitz, C. H. *J. Phys. Chem. B* **2011**, *115*, 2447. (b) Mukherjee, P. S.; Lopez, N.; Arif, A. M.; Cervantes-Lee, F.; Noveron, J. *Chem. Commun.* **2007**, 1433. (c) Guzei, I. A.; Mitra, A.; Spencer, L. C. *Cryst. Growth Des.* **2009**, *9*, 2287. (d) Marucci, A.; Launois, P.; Moret, R.; Pénicaud, A. *Eur. Phys. J. B* **2002**, *26*, 29. (e) Grepioni, F.; Cojazzi, G.; Draper, S. M.; Scully, N.; Braga, D. *Organometallics* **1998**, *17*, 296. (f) Avarvari, N.; Faulques, E.; Fourmigué, M. *Inorg. Chem.* **2001**, *40*, 2570. (g) Henderson, W. A.; Young, V. A.; Passerini, S.; Truelove, P. C.; De Long, H. C. *Chem. Mater.* **2006**, *18*, 934.

(19) (a) Allendorf, M. D.; Bauer, C. A.; Bhakta, R. K.; Houk, R. J. T. *Chem. Soc. Rev.* **2009**, *38*, 1330, and references therein. (b) Yang, Y.; Zeng, M.-H.; Zhang, L.-J.; Liang, H. *J. Coord. Chem.* **2009**, *62*, 886.

(20) (a) Huang, Z.; White, P.; Brookhart, M. *Nature* **2010**, *465*, 598. (b) Shimomura, S.; Matsuda, R.; Kitagawa, S. *Chem. Mater.* **2010**, *22*, 4129. (c) Mir, M. H.; Koh, L. L.; Tan, G. K.; Vittal, J. J. *Angew. Chem., Int. Ed.* **2010**, *49*, 390. (d) Ghosh, S.; Kaneko, W.; Kiriya, D.; Ohba, M.; Kitagawa, S. *Angew. Chem., Int. Ed.* **2008**, *47*, 8843. (e) Vittal, J. J. *Coord. Chem. Rev.* **2007**, *251*, 1781. (f) Kaneko, W.; Ohba, M.; Kitagawa, S. *J. Am. Chem. Soc.* **2007**, *129*, 13706. (g) Kawano, M.; Fujita, M. *Coord. Chem. Rev.* **2007**, *251*, 2592. (h) Zheng, S.-Z.; Messerschmidt, M.; Coppens, P. *Chem. Commun.* **2007**, 2735. (i) Neville, S. M.; Halder, G. J.; Chapman, K. W.; Duriska, M. B.; Southon, P. D.; Cashion, J. D.; Letard, J.-F.; Moubaraki, B.; Murray, K. S.; Kepert, C. J. *J. Am. Chem. Soc.* **2008**, *130*, 2869. (j) Halder, G. J.; Kepert, C. J. *Aus. J. Chem.* **2006**, *59*, 597 and references therein.